

## DIFFUSION-WEIGHTED MR IMAGING: ROLE IN THE DIFFERENTIAL DIAGNOSIS OF BREAST LESIONS

C. Altay<sup>1</sup>, P. Balci<sup>1</sup>, S. Altay<sup>2</sup>, S. Karasu<sup>2</sup>, S. Saydam<sup>3</sup>, T. Canda<sup>4</sup>, O. Dicle<sup>1</sup>

**Purpose:** To evaluate the diagnostic value of magnetic resonance diffusion-weighted imaging (DWI) using apparent diffusion coefficient (ADC) values to the characterization of breast lesions and differentiation of benign and malignant lesions.

**Materials and methods:** Thirty-seven women (mean age, 38 years) with 37 enrolled in the study. DWI and ADC maps in the axial plane were obtained using a 1.5 Tesla MRI device. Mean ADC measurements were calculated among cysts, normal fibroglandular tissue, benign lesions and malignant lesions were evaluated.

**Results:** Out of 37 women, 4 had normally breast MRI findings. The diagnosis of remaining 33 patients with 37 breast lesions were as follows; malign lesions (n = 23), benign lesions (n = 10) and simple breast cyst (n = 4). The ADC values were as follows (in units of  $10^{-3}$  mm<sup>2</sup>/s): Normal fibroglandular tissue (range: 1.39-2.06; mean:  $1.61 \pm 0.23$ ), benign breast lesions (range: 1.09-1.76; mean:  $1.47 \pm 0.25$ ), cysts (range: 2.27-2.46, mean:  $2.37 \pm 0.07$ ) and malignant breast lesions (range: 0.78-1.26, mean:  $0.96 \pm 0.25$ ). The mean ADC obtained from malignant breast lesions was statistically different from that observed in benign solid lesions ( $p < 0.01$ ) and normal fibroglandular breast tissue ( $p < 0.01$ ). Furthermore, the mean ADC values of benign breast lesions was not statistically different from cyst ( $p \geq 0.01$ ) and normal fibroglandular breast tissue ( $p \geq 0.01$ ). A ADC value of  $1.1 \times 10^{-3}$  mm<sup>2</sup>/s as a threshold value provided differentiation for malign and benign lesions, with a sensitivity of 91.3% and a specificity of 85.7% compared with conventional breast MRI values.

**Conclusion:** DWI with quantitative ADC measurements is a reliable tool for differentiation of benign and malignant breast lesions.

**Key-word:** Breast neoplasms, MR.

Currently mammography and ultrasonography still represents the primary imaging modalities used for breast cancer screening and diagnosis (1). Breast magnetic resonance imaging (MRI) is the problem solving method for the diagnosis of breast cancer (2). The conventional dynamic breast MRI has shown diagnostic sensitivities of 94–99% for invasive breast cancer, whereas various specificities have been reported (37–86%) (3, 4). Diffusion-weighted imaging (DWI) is a useful method for the detection, diagnosis and staging of breast cancer. To increase the specificity of breast MRI, DWI could contribute to the correct diagnosis of breast lesions.

DWI is a technique that acquires an image during a single breath-hold and does not require contrast agent (5). DWI provides potentially exclusive information on the viability and cellularity of the in vivo tissue. It provides image contrast that is dependent on the molecular motion of water, which may be substantially altered by disease and tissue. Over

time, several studies on breast and abdominal organs examined with DWI were published (6-12). In these studies it was shown that apparent diffusion coefficient (ADC) values of normal tissues and lesions can be measured using diffusion-weighted images, and the differences in ADC values can be used in the differential diagnosis.

The major aim of the current study was to measure the ADC values of benign and malignant breast lesions using DWI and to determine their contribution to differential diagnosis.

### Materials and methods

#### Patients

The study included conscious adult patient volunteers over 18 years of age with breast lesions that were detected by mammography or ultrasonography having a diameter > 1 cm in our department. All patients gave their written informed consent prior to participating in the study, which had been ap-

proved by the local institutional review board. We joined in a prospective clinical trial 37 women (age range: 22–74 years; mean age: 47 years) with 37 breast lesions. Ethical approval of the study was obtained (Fig. 1, 2).

#### MRI

Conventional breast MR imaging, and DWI in a 1.5 T superconductor scanner (Intera, Gyroscan, Philips, Best, Holland) using a dedicated bilateral breast coil (four-channel breast array coil) consisting of 4 coil elements with 4 integrated preamplifiers. All patients underwent imaging in the prone position. A localizing sequence was followed by axial fast spin-echo T2-weighted imaging (repetition time (TR), 5056 ms; echo time (TE), 120 ms; echo train length, 15; section thickness, 4 mm; intersection spacing, 0,8 mm; matrix size, 256 x 256; field of view, 30 cm) with fat suppression spectral presaturation inversion recovery and fast spin-echo T1-weighted imaging (TR, 550 ms; TE, 11 ms; echo train length, 15; section thickness, 4 mm; intersection spacing, 0,8 mm; matrix size, 256 x 256; field of view, 30 cm) with fat suppression (principle of selective excitation technique). This examination was followed by a dynamic study of the both of breast that consisted of serial imaging with a three-dimensional axial fast field echo T1-weighted sequence (FFE 3D; TR, 15 ms; TE, 5 ms; flip angle, 30°;

*From:* 1. Department of Radiology, Dokuz Eylul University, Faculty of Medicine, Izmir, Turkey, 2. Department of Radiology, Izmir Atatürk Research and Training Hospital, Izmir, Turkey, 3. Department of General Surgery, Dokuz Eylul University, Faculty of Medicine, Izmir, Turkey, 4. Department of Pathology, Dokuz Eylul University, Faculty of Medicine, Izmir, Turkey.

*Address for correspondence:* Dr C. Altay, M.D., Dokuz Eylul University, Faculty of Medicine, Department of Radiology, Mithatpaşa Cad. Inciralti 35340 Izmir, Turkey. E-mail: cananalay@yahoo.com

section thickness, 2 mm; intersection spacing, 0.4 mm; matrix size, 256 × 256; field of view, 30 cm; acquisition time 1 min per measurement) with fat suppression (principle of selective excitation technique). After the first acquisition, intravenous bolus injection of 0.1 mmol/kg body weight gadopentetate dimeglumine (Gd-DTPA, Magnevist, Bayer HealthCare, Leverkusen, Germany) at a flow rate of 3 ml/s by an automatic injector (Spectris, Medrad, Pittsburgh, USA) was performed, followed immediately by 20 ml of a saline solution. Thirty seconds after contrast agent injection, dynamic MR imaging was continued, using the same sequence parameters and tuning conditions, for a total of 7 contrast-enhanced measurements. The imaging timing of the dynamic series included pre-contrast, early arterial, delayed arterial, venous, and equilibrium phases of the breast. Subtraction of multiphasic contrast enhanced dynamic series was automatically acquired by the software of MR device. The software provided a new series by image-by-image subtraction of pre-contrast series from each post-contrast series of each patient. DWI studies were performed before contrast enhanced images were obtained. Diffusion-weighted sequences (TR/TE, 4200/95 ms; flip angle, 90°; slice thickness, 5 mm; field of view, 230 × 230 mm; matrix, 256 × 256; breath-holding time, 50 s) in the transverse plane were performed, applying gradients (in order to sensitize SE sequence to diffusion) to single-shot echo-planar sequences in all 3 axes (x, y, z), and 2 different b values (b = 0 s/mm<sup>2</sup> and b = 1000 s/mm<sup>2</sup>). ADC maps were formed with these images.

The measurements were made using by a circular region of interest (ROI) 10 mm in diameter in the target lesion and normal breast area on the ADC maps with reference to conventional MRI. In large-sized lesions the mean value of three different ROI measurements on the same slice was calculated. The measurements were performed from contrast enhanced solid parts on conventional breast MRI sequences and post-contrast images especially for heterogeneous lesions. In small-sized lesions the ADC value calculated with using a single ROI.

#### Statistical analysis

Pairwise comparisons for groups of more than 1 were performed using the Mann-Whitney *U* test with Benferroni correction for multiple

comparisons. ADC values were compared between malignant and benign masses using the Mann-Whitney *U* test. Statistical analysis was performed with SPSS software (Statistical Package for the Social Sciences, Version 16.0.2; SPSS, Chicago, Ill). A *P* value of less than 0.05 was considered as a statistically significant difference.

## Results

### Conventional breast MRI findings and demographics of patients

The conventional breast MR images in 37 patients reviewed by using the Breast Imaging Reporting and Data System (BI-RADS) MR lexicon (13) by two radiologists (C.A. and P.B., with 5 and 13 years of breast MR imaging experience, respectively). All 37 lesions were included in category 4a (*n* = 12), category 4b (*n* = 17), or category 5 (*n* = 8) with conventional breast MRI findings.

The histopathologic diagnosis was obtained for all 37 lesions. The benign breast lesions included fibroadenomas (4/37, 10.8%), hamartoma (1/37, 2.7%), cysts (4/37, 10.8%), granulation tissue without underlying lesion in the region prior to surgery (2/37, 5.4%), sclerosing adenosis (1/37, 2.7%), ductal ectasia (1/37, 2.7%), and early stage fat necrosis (1/37, 2.7%). The malignant breast lesions were invasive ductal carcinomas (9/37, 24.3%), invasive lobular carcinomas (6/37, 16.2%), mixed type invasive ductal and lobular carcinomas (4/37, 10.8%), medullary carcinoma (1/37, 2.7%), and malignant epithelial tumor (1/37, 2.7%). Final diagnosis included 4 cysts, 10 benign solid lesions and 23 malignant lesions. The mean size of cysts, benign lesions and malignant lesions and was, respectively, 1.7 cm (range, 1.6-2.3 cm), 2.9 cm (range, 1.9-6.4 cm), 2.9 cm (range, 1.5-13.5 cm).

### Diffusion weighted MR imaging findings

The powerful significant difference in the median ADC value of benign breast lesions (median,  $1.47 \pm 0.25 \times 10^{-3}$  mm<sup>2</sup>/s; range, 1.09–1.76 × 10<sup>-3</sup> mm<sup>2</sup>/s) compared with malignant breast masses ( $0.96 \pm 0.25 \times 10^{-3}$  mm<sup>2</sup>/s; 0.78-1.26 × 10<sup>-3</sup> mm<sup>2</sup>/s) was obtained (*p* < 0.01). The median ADC values of different lesion types are shown in Table II. The median ADCs of cysts ( $2.37 \pm 0.07 \times 10^{-3}$  mm<sup>2</sup>/s; 2.27-2.46 × 10<sup>-3</sup> mm<sup>2</sup>/s) were significantly differ-

ent from the malignant breast lesions (*p* = 0,006) and normal fibroglandular breast tissue ( $1.61 \pm 0.23 \times 10^{-3}$  mm<sup>2</sup>/s; 1.39–2.06 × 10<sup>-3</sup> mm<sup>2</sup>/s) (*p* = 0,004). There was no statistically significant difference between benign breast lesions and normal fibroglandular breast tissue (*p* > 0,01).

There was no difference in ADC values among benign breast lesions including fibroadenomas ( $1.45 \pm 0.17 \times 10^{-3}$  mm<sup>2</sup>/s; 1.06-1.58 × 10<sup>-3</sup> mm<sup>2</sup>/s), cysts ( $2.37 \pm 0.07 \times 10^{-3}$  mm<sup>2</sup>/s; 2.37-2.46 × 10<sup>-3</sup> mm<sup>2</sup>/s), granulation tissues ( $1.41 \pm 0.27 \times 10^{-3}$  mm<sup>2</sup>/s; 1.24-1.48 × 10<sup>-3</sup> mm<sup>2</sup>/s), fat necrosis ( $1.39 \times 10^{-3}$  mm<sup>2</sup>/s), hamartoma ( $1.64 \times 10^{-3}$  mm<sup>2</sup>/s), sclerosing adenosis ( $1.76 \times 10^{-3}$  mm<sup>2</sup>/s) and ductal ectasia ( $1.38 \times 10^{-3}$  mm<sup>2</sup>/s) (Table I). The mean ADC value of each type of lesion was invasive ductal carcinoma:  $0.95 \times 10^{-3}$  mm<sup>2</sup>/s, DCIS:  $0.98 \times 10^{-3}$  mm<sup>2</sup>/s. The malignant breast masses in this study could not be differentiated using DWI, and ADC values of invasive ductal carcinomas were  $0.94 \times 10^{-3}$  mm<sup>2</sup>/s (0.88-0.98 × 10<sup>-3</sup> mm<sup>2</sup>/s); invasive lobular carcinomas,  $0.79 \times 10^{-3}$  mm<sup>2</sup>/s (0.89-1.09 × 10<sup>-3</sup> mm<sup>2</sup>/s); ductal carcinoma in situ,  $0.98 \times 10^{-3}$  mm<sup>2</sup>/s (0.87-1.26 × 10<sup>-3</sup> mm<sup>2</sup>/s); and the single case of medullary carcinoma,  $0.92 \times 10^{-3}$  mm<sup>2</sup>/s and malignant epithelial tumor,  $1.18 \times 10^{-3}$  mm<sup>2</sup>/s (Table II).

On DWI, all malignancies had ADC ≤ 1.1 × 10<sup>-3</sup> mm<sup>2</sup>/s in our study. Using a mean ADC of > 1.1 provided a sensitivity of 91.3%, a specificity of 85.7%, and an accuracy of 89.1% to designation lesions as benign.

## Discussion

Conventional breast MRI is the widely used diagnostic technique for evaluating the different breast disease (1). To increase the detectability of breast cancer, several techniques are used for breast MRI. Especially, dynamic-enhanced MRI provides for evaluating suspicious breast lesions and it has a very high sensitivity for defining breast cancer (14). Although, dynamic-enhanced breast MRI has some limitations such as it has a long relative lower specificity compared to conventional breast imaging methods (15,16).

A diffusion-weighted sequence was first described by Stejskal and Tanner in 1965 (11). In the practice commonly used is an ultrafast spin echo echoplanar T2-weighted sequence. For a long time, this imaging technique has been used only for neuroradiology. Recently, increased use of DWI in practice for the

Table I. — Distribution of mean ADC values in histologic types of cystic and solid benign lesions.

Benign cystic and solid lesions	n	Mean ADC value ( $10^{-3}$ mm <sup>2</sup> /s)
Fibroadenoma	4	1.45 ± 0.17
Granulation (after surgery)	2	1.41 ± 0.27
Ductal ectasia	1	1.38
Sclerosing adenosis	1	1.76
Hamartoma	1	1.64
Fat necrosis	1	1.39
Cyst	4	2.37 ± 0.07
Total	14	

Table II. — Distribution of mean ADC values in histologic types of breast cancer.

Malignant lesions	n	Mean ADC value ( $10^{-3}$ mm <sup>2</sup> /s)
Invasive ductal carcinoma		
Solid tubular Ca	9	0.94 ± 0.29
Lobular Ca	6	0.79 ± 0.36
Medullary Ca	1	0.92
Malign epithelial Ca	1	1.18
Ductal carcinoma in situ	4	0.98 ± 0.26
Total	21	

evaluation of benign and malignant tumors in the body such as pancreatic, uterus, hepatic, prostate and breast tumors (17, 18, 19, 20).

Diffusion is the term used for the randomized microscopic movement of molecules which is known as Brownian motion and this movement is measured from mean diffusion coefficient. DWI is sensitive to this randomized movement that is measured with ADC (21). ADC mea-

surements could be affected by several factors including cellularity, permeability, capillary perfusion, temperature, magnetic sensitivity of the tissue, and motion affects the actual diffusion. DWI can be performed after strong bipolar radiofrequencies pulses are added to spin echo or gradient echo sequences, by sensitizing the molecules in tissue to diffusion. Therefore, the microscopic movement of molecules can be evaluated

in vivo. In vivo, the diffusion of water molecules is restricted due to macromolecules and membranes. Highly cellular tissues provides decreased to diffusion. Conversely, it increases with crashed membranes or in low cellular tissues. DWI may be evaluated quantitatively by ADC values.

There are some limitations of DWI. The EPI based pulse sequence was used in the present study. EPI-DWI has technical limitations such as poor spatial resolution and the potential risk of image distortion caused by post-operation clips material which results in magnetic field inhomogeneity, patient motion, and tissue-air interface. Other DWI techniques based on parallel line scan (Periodically rotated overlapping parallel lines with enhanced reconstruction- PROPELLER sequence) diffusion (18) or on the addition of parallel imaging (sensitivity encoding-SENSE sequence) diffusion (22) can help reduce distortion and may help further improve diagnostic accuracy.

In this study, ADC measurements of benign and malignant breast tumors were significantly different, so that compatible with findings of previous studies (6-12). Cysts, normal fibroglandular breast tissue, and benign breast tumors had the highest ADC values, although malignant breast masses had the lowest. There are many studies of benign and malignant masses discrimination of the breast. The findings of studies show that the mean ADC values of the malignant tumors were  $1.60 \pm 0.36 \times 10^{-3}$  mm<sup>2</sup>/s using b value with 400 by Sinha et al. (14),  $1.22 \pm 0.19 \times 10^{-3}$  mm<sup>2</sup>/s using b value with 700 by Kinoshita et al. (13),

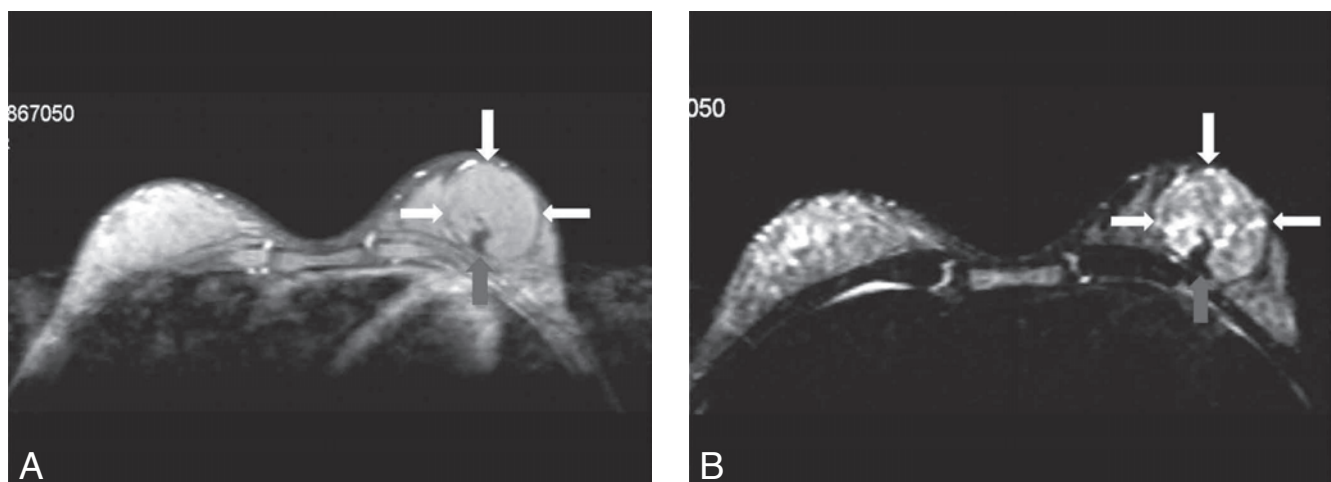


Fig. 1. — A. Transverse fat saturated T1-weighted turbo spin-echo MR image (SPIR TSE T1) from a 49-year-old female patient with a histologically proved hamartoma in the left breast (white arrows). B. The fat saturated T2-weighted image (SPIR TSE T2) also shows a slowly bright signal intensity of the lesion (arrows) with a small amount fat tissue is marked with a grey arrow in Fig. 1 A-E.

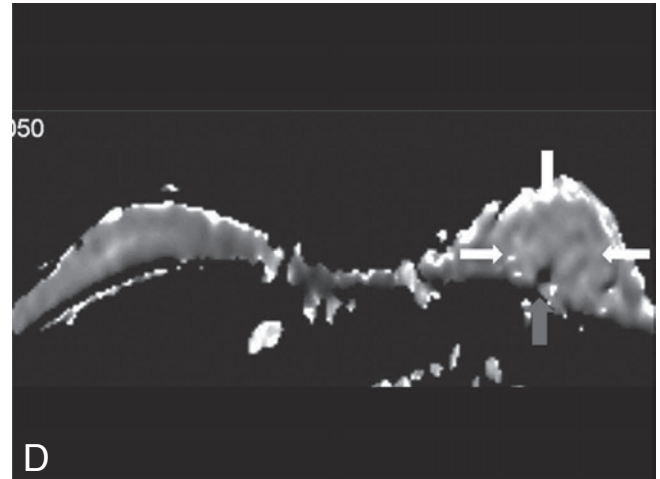
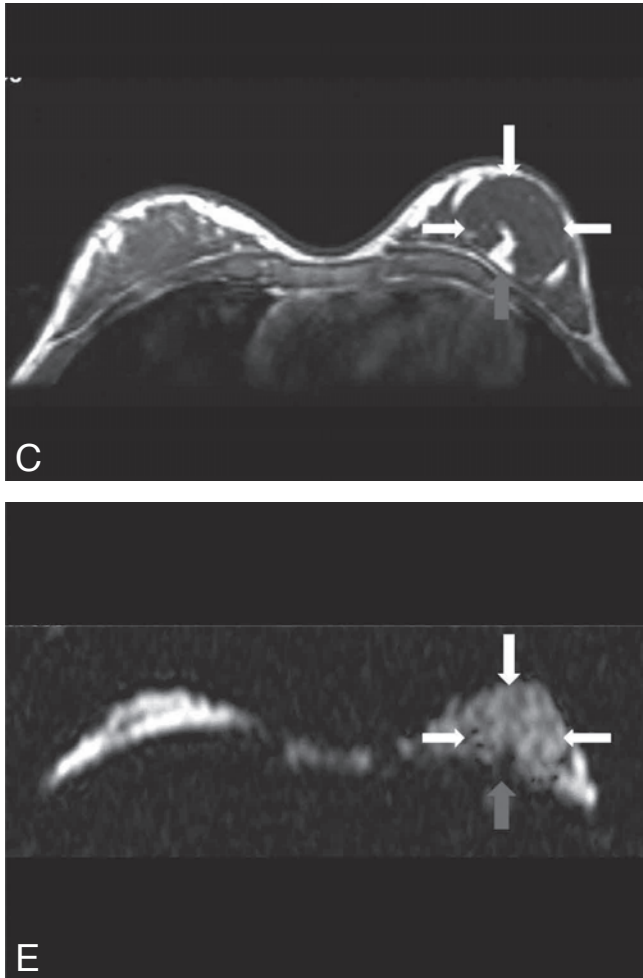


Fig. 1. — C. The T1-weighted gradient-echo image (3D FFE) also shows a iso-intense lesion compared with normal breast tissue (white arrows). D. Diffusion-weighted image ( $b = 1,000 \text{ mm}^2/\text{s}$ ) reveals slightly hypointensity of the mass with more clear borders (arrows). E. Apparent diffusion coefficient (ADC) was calculated. Tumor on ADC image shows isointense compared with normal parenchyma.

$1.12 \pm 0.24 \times 10^{-3} \text{ mm}^2/\text{s}$  using  $b$  value with 750 by Woodhams et al. (17),  $1.25 \pm 0.29 \times 10^{-3} \text{ mm}^2/\text{s}$  using  $b$  value with 600 by Marini et al. (16), and  $0.97 \pm 0.20 \times 10^{-3} \text{ mm}^2/\text{s}$  using  $b$  value with 1000 by Guo et al. (15).

Twenty-three malignant lesions in our study had ADC values  $0.92 \pm 0.25 \times 10^{-3} \text{ mm}^2/\text{s}$  ( $b$  value was chosen 1000), which is well correlated with the similar  $b$  value study results. Also, the mean ADC value of normal

breast tissues ( $1.61 \pm 0.23 \times 10^{-3} \text{ mm}^2/\text{s}$ ) in this study was comparable with reported ADC values of  $1.63 \pm 0.22 \times 10^{-3} \text{ mm}^2/\text{s}$  by Guo et al. (15). Guo et al. were selected the  $b$  value = 1000 so this is similar to our study. They demonstrated 93% sensitivity with the threshold  $1.3 \times 10^{-3} \text{ mm}^2/\text{s}$  of ADC value for differentiated malignant and benign lesions (8). Although, our study showed a 91.3% sensitivity to breast cancer with a threshold of  $1.1 \times 10^{-3} \text{ mm}^2/\text{s}$  (Table III).

Compared to the prior reports, our benign breast tumors had highest ADC values of, which were similar to

Table III. — Comparison of previous studies about diffusion imaging of breast lesions. "n": number of case; \*:  $\times 10^{-3} \text{ mm}^2/\text{s}$ ; Sens: sensitivity; Spec: specificity.

Previous studies	«n»	«b» value	Mean ADC* value of benign tumours	Mean ADC* value of breast cysts	Mean ADC* value of malignant tumours	ADC* of normal breast tissue	Cut of value of ADC*	Sens. %	Spec. %
Kinoshita et al.	21	700	$1.49 \pm 0.18$	$1.21 \pm 0.18$	–	–	–	–	–
Sinha et al.	23	400	$2.01 \pm 0.46$	$2.65 \pm 0.30$	$1.60 \pm 0.36$	$2.37 \pm 0.27$	–	–	–
Guo et al.	52	1000	$1.57 \pm 0.23$	$2.35 \pm 0.08$	$0.97 \pm 0.20$	–	1.3	93	88
Marini et al.	91	600	$1.74 \pm 0.46$	$2.25 \pm 0.26$	$1.25 \pm 0.29$	–	–	–	–
Woodhams et al.	31	750	$1.74 \pm 0.46$	$2.25 \pm 0.26$	$1.12 \pm 0.24$	$2.05 \pm 0.27$	1.6	93	46
Current study	37	1000	$1.74 \pm 0.25$	$2.37 \pm 0.07$	$0.96 \pm 0.25$	$1.61 \pm 0.23$	1.1	91.3	85.7

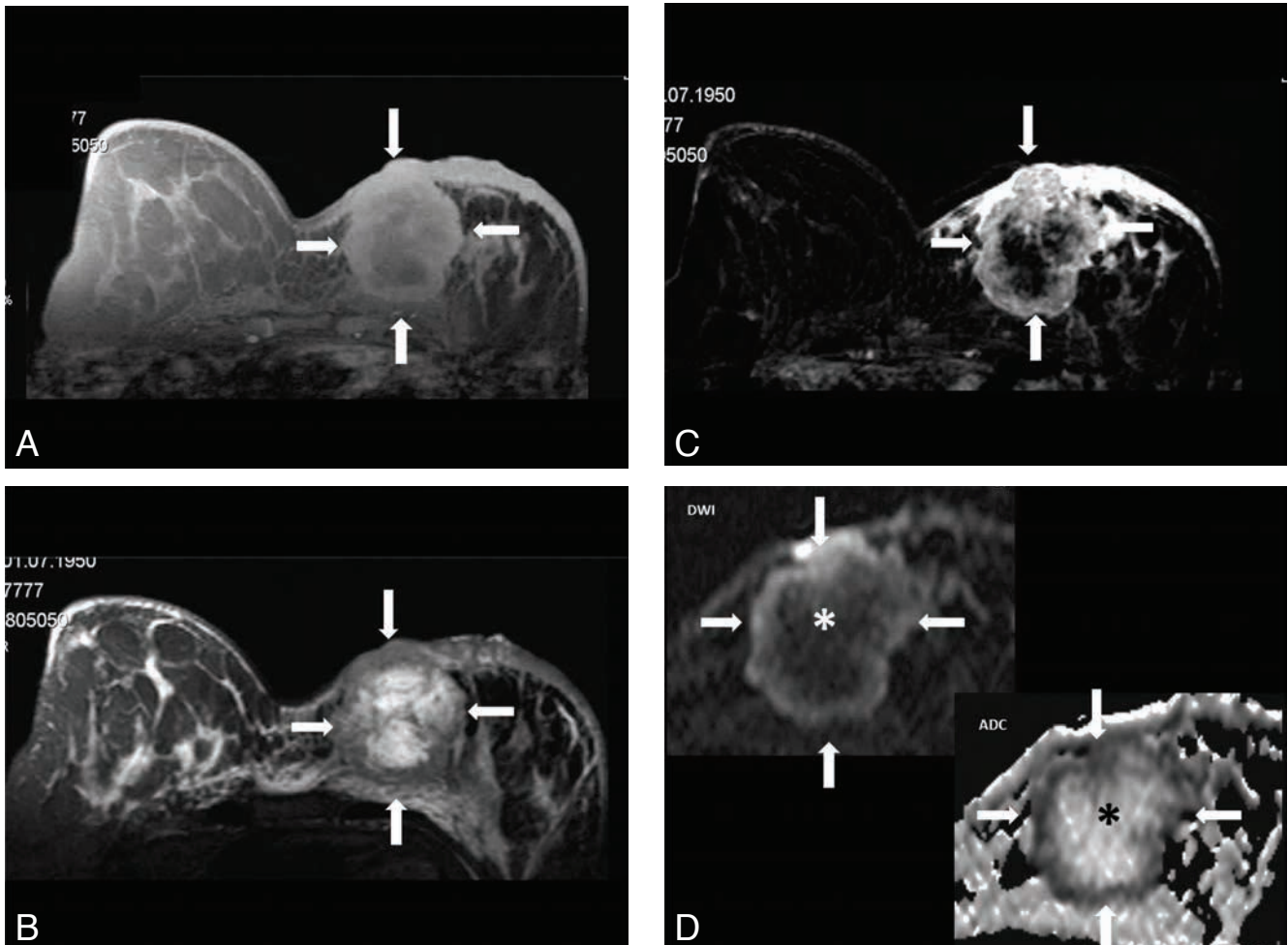


**Fig. 2.** — A. Transverse fat saturated T1-weighted turbo spin-echo MR image (SPIR TSE T1) from a 52-year-old female patient with a histologically proved invasive lobular carcinoma in the left breast (arrows). The mass shows slightly high signal intensity compared with right breast glandular tissue. B. The corresponding fat saturated T2-weighted image (SPIR TSE T2) has a bright lesion within the left breast (arrows) and there is diffuse thickening and edema of the ipsilateral breast skin in Fig. 2 A-C. C. Contrast-enhanced T1-weighted 3D fast field-echo axial image (3D FFE) in early phase submitted to subtraction shows peripherally enhanced mass (arrows) and central cystic component (asterisks). D. Diffusion-weighted image ( $b = 1,000 \text{ mm}^2/\text{s}$ ) shows a left breast mass (arrows) with solid and cystic components. Apparent diffusion coefficient (ADC) reveals restricted diffusion (arrows) in the solid component and increased diffusion (asterisks) in the cystic part of the mass.

ADC values of benign breast tumors in our study. The mean ADC values of the 4 simple cysts were  $2.37 \pm 0.07 \times 10^{-3} \text{ mm}^2/\text{s}$ . These results were consistent with ADC values observed in past studies.

The ADC values of the tumors were significantly correlated with tumor cellularity. Intracranial primary tumors such as gliomas and meningiomas manifested a good correlation between the ADC value and tumor cellularity (23). Low-grade tumors tend to have higher ADC values than those of high-grade tumors, which may reflect the increase of water content within the neoplastic cells or interstitial spaces. Investigators noted that tumor cellularity was inversely correlated with ADC values of tumor. In tumors, the ADC value is highest in areas of cystic necrosis,

followed by vasogenic peritumoral edema, nonenhancing solid tumor, and enhancing solid-tumor components (24). The high cellularity typical of some benign breast lesions (intraductal papilloma and fibrocystic mastopathy) has been responsible (11-13) as the possible cause of false positive DWI findings. In our study, we had one false positive case (fibroadenoma; ADC value  $1.06 \times 10^{-3} \text{ mm}^2/\text{s}$ ) using the threshold of  $1.1 \times 10^{-3} \text{ mm}^2/\text{s}$ .

There are some causes affects to the ADC values in different studies. In the study which has been used low  $b$ -value DWI (in low diffusion weighting) all masses were observed as hyperintense due to T2 effect (14), whereas on high  $b$ -value studies (in high diffusion weighting) signals of masses obviously decreased due to

diffusion restriction (15,16). Although true diffusion is independent of field strength, ADC values are affected by microscopic perfusion and artifacts due to field inhomogeneity; thus, ADC values are typically lower by 2–10% at 3 T compared with values at 1.5 T (25). The choice of  $b$  values also affects the calculated ADCs, with the use of higher  $b$  values ( $> 500 \text{ mm}^2/\text{s}$ ) being more accurate for true diffusion and resulting in lower ADC values (17).

Other methods of cancer detection in the breast include MR spectroscopy and dynamic contrast-enhanced MRI, with many of the published articles in the literature. The studies with dynamic contrast-enhanced MRI have shown a variable sensitivity and specificity. In contrast to these methods, DWI has

the advantages of not requiring IV contrast material and of being simple to process. Moreover, DWI requires less time to acquire than proton spectroscopy and less technologist training to perform. Furthermore, diffusion tensor MRI used to evaluate breast tumors. Baltzer et al. were emphasized that not only mean diffusivity but also diffusion anisotropy significantly differs between different breast neoplasms (12).

Our study had several limitations. First, the relatively small sample size of our study. Second limitation was the low spatial resolution due to high b value selection with using EPI sequence, especially in small breast lesions (< 1 cm). Third, ADC values were manually calculated by two radiologists. Inter- and intra-observer differences were not excluded. Finally, we did not compare the utility of conventional breast MR with DWI.

## Conclusion

The diffusion-weighted MRI sequence is a useful diagnostic tool since it can be obtained short time, there is no need to use contrast agent. It can contribute to accurate diagnosis when discrimination of benign and malignant breast masses when use with conventional MRI sequences. DWI is likely to be particularly useful with those in whom the use of gadolinium is contraindicated. In addition, the DWI can be effective screening technique in the patients with suspicious conventional breast imaging findings.

## References

- Swedish Organised Service Screening Evaluation Group. Reduction in breast cancer mortality from the organised service screening with mammography: validation with alternative analytic methods. *Cancer Epidemiol Biomarkers Prev*, 2006, 15: 52-56. (PMID: 16434586)
- Warner E., Messersmith H., Causer P., Eisen A., Shumak R., Plewes D.: Systematic review: using magnetic resonance imaging to screen women at high risk for breast cancer. *Ann Intern Med*, 2008, 148: 671-679. (PMID: 18458280)
- Orël S.G., Schnall M.D.: MR imaging of the breast for the detection, diagnosis, and staging of breast cancer. *Radiology*, 2001, 220: 13-30. (PMID: 11425968)
- Kuhl C.K., Mielcareck P., Klaschik S., Leutner C., Wardelmann E., Gieseke J., et al.: Dynamic breast MR imaging: are signal intensity time course data useful for differential diagnosis of enhancing lesions? *Radiology*, 1999, 211: 101-110. (PMID: 10189459)
- Woodhams R., Ramadan S., Stanwell P., Sakamoto S., Hata H., et al.: Diffusion-weighted imaging of the breast: Principles and clinical applications. *Radiographics*, 2011, 31: 1059-1084.
- Kinoshita T., Yashiro N., Ihara N., Funatu H., Fukuma E., Narita M.: Diffusion-weighted half-Fourier single-shot turbo spin echo imaging in breast tumors: differentiation of invasive ductal carcinoma from fibroadenoma. *J Comput Assist Tomogr*, 2002, 26: 1042-1046. (PMID: 12488758)
- Sinha S., Lucas-Quesada FA., Sinha U., DeBruhl N., Bassett L.W.: In Vivo Diffusion-Weighted MRI of the Breast: Potential for Lesion Characterization. *J Magn Reson Imaging*, 2002, 15: 693-704. (PMID: 12112520)
- Guo Y., Cai Y.Q., Cai Z.L., Gao Y.G., An N.Y., Ma L., et al.: Differentiation of clinically benign and malignant breast lesions using diffusion-weighted imaging. *J Magn Reson Imaging*, 2002, 16: 172-178. (PMID: 12203765)
- Marini C., Iasconi C., Giannelli M.: Quantitative diffusion-weighted MR imaging in the differential diagnosis of breast lesion. *Eur Radiol*, 2007, 17: 2646-2655. (PMID: 17356840)
- Woodhams R., Matsunaga K., Iwabuchi K., Kan S., Hata H., Kuranami M., et al.: Diffusion-weighted imaging of malignant breast tumors: the usefulness of apparent diffusion coefficient (ADC) value and ADC map for the detection of malignant breast tumors and evaluation of cancer extension. *J Comput Assist Tomogr*, 2005, 29: 644-649. (PMID: 16163035)
- Tozaki M., Fukuma E.: H<sup>1</sup> MR Spectroscopy and Diffusion-Weighted Imaging of the Breast: Are They Useful Tools for Characterizing Breast Lesions Before Biopsy? *AJR Am J Roentgenol*, 2009, 193: 840-849. (PMID: 19696300)
- Baltzer P.A.T., Schäfer A., Dietzel M., Grässel D., Gajda M., Camara O., et al.: Diffusion tensor magnetic resonance imaging of the breast: a pilot study. *Eur Radiol*, 2011, 21: 1-10. (PMID: 20668860)
- American College of Radiology. Breast imaging reporting and data system (BI-RADS) - MRI. 1st ed. Reston, Va: American College of Radiology, 2003.
- Bluemke D.A., Gatsonis C.A., Chen M.H., DeAngelis G.A., DeBruhl N., Harms S., et al.: Magnetic resonance imaging of the breast prior to biopsy. *JAMA*, 2004, 292: 2735-2742. (PMID: 15585733)
- Ikeda D.M., Baker D.R., Daniel B.L.: Magnetic resonance imaging of breast cancer: clinical indications and breast MRI reporting system. *J Magn Reson Imaging*, 2000, 12: 975-983. (PMID: 11105039)
- Le Bihan D., Turner R., Douek P., Patronas N.: Diffusion MR imaging: clinical applications. *AJR Am J Roentgenol*, 1992, 159: 591-599. (PMID: 1503032)
- Koh D.M., Collins D.J.: Diffusion-weighted MRI in the body: applications and challenges in oncology. *AJR Am J Roentgenol*, 2007, 188: 1622-1635. (PMID: 17515386)
- Chan I., Wells W. 3rd., Mulhern R.V., Haker S., Zhang J., Zou K.H., et al.: Detection of prostate cancer by integration of line-scan diffusion, T2-mapping and T2-weighted magnetic resonance imaging: a multichannel statistical classifier. *Med Phys*, 2003, 30: 2390-2398. (PMID: 14528961)
- Kono K., Inoue Y., Nakayama K., et al.: The role of diffusion-weighted imaging in patients with brain tumors. *AJNR Am J Neuroradiol*, 2001, 22: 1081-1088. (PMID: 11415902)
- Le Bihan D., Douek P., Argyropoulou M.: Diffusion and perfusion magnetic resonance imaging in brain tumors. *Top Magn Reson Imaging*, 1993, 5: 25-31. (PMID: 8416686)
- Le Bihan D., Breton E., Lallemand D., Grenier P., Cabanis E., Laval-Jeantet M.: MR Imaging of intravoxel incoherent motions: application to diffusion and perfusion in neurologic disorders. *Radiology*, 1986, 161: 401-407. (PMID: 3763909)
- Liu C., Moseley M.E., Bammer R.: Simultaneous phase correction and SENSE reconstruction for navigated multi-shot DWI with non-cartesian k-space sampling. *Magn Reson Med*, 2005, 54: 1412-1422. (PMID: 16276497)
- Sugahara T., Korogi Y., Kochi M., Ikushima I., Shigematu Y., Hirai T., et al.: Usefulness of diffusion weighted MRI with echo-planar technique in the evaluation of cellularity in gliomas. *J Magn Reson Imaging*, 1999, 9: 53-60. (PMID: 10030650)
- Huisman T.A., Loenneker T., Barta G., Bellemann M.E., Hennig J., Fischer J.E., et al.: Quantitative diffusion tensor MR imaging of the brain: field strength related variance of apparent diffusion coefficient (ADC) and fractional anisotropy (FA) scalars. *Eur Radiol*, 2006, 16: 1651-1658. (PMID: 16532356).